ACS OMEGA

http://pubs.acs.org/journal/acsodf

Article

σ-Hole and LP-Hole Interactions of Pnicogen···Pnicogen Homodimers under the External Electric Field Effect: A Quantum Mechanical Study

Mahmoud A. A. Ibrahim,* Nayra A. M. Moussa, Sherif M. A. Saad, Muhammad Naeem Ahmed, Ahmed M. Shawky, Mahmoud E. S. Soliman, Gamal A. H. Mekhemer, and Al-shimaa S. M. Rady

Cite This: *ACS Omega* 2022, 7, 11264−11275

Read Online

ACCESS | Metrics & More | Article Recommendations

ABSTRACT: σ-Hole and lone-pair (lp)-hole interactions within σ-hole···σ-hole, σ-hole···lp-hole, and lp-hole···lp-hole configurations were comparatively investigated on the pnicogen···pnicogen homodimers $(PCl_3)_2$, for the first time, under field-free conditions and the influence of the external electric field (EEF). The electrostatic potential calculations emphasized the impressive versatility of the examined PCl_3 monomers to participate in σ-hole and lp-hole pnicogen interactions. Crucially, the sizes of σ-hole and lp-hole were enlarged under the influence of the positively directed EEF and decreased in the case of reverse direction. Interestingly, the energetic quantities unveiled more favorability of the σ-hole···lp-hole configuration of the pnicogen···pnicogen homodimers, with significant negative interaction energies, than σ-hole···σ-hole and lp-hole···lp-hole configurations. Quantum theory of atoms in molecules and noncovalent interaction index analyses were adopted to elucidate the nature and origin of the considered interactions, ensuring their closed shell nature and the occurrence of attractive forces within the studied homodimers. Symmetry-adapted perturbation theory-based energy decomposition analysis alluded to the dispersion force as the main physical component beyond the occurrence of the examined interactions. The obtained findings would be considered as a fundamental underpinning for forthcoming studies pertinent to chemistry, materials science, and crystal engineering.

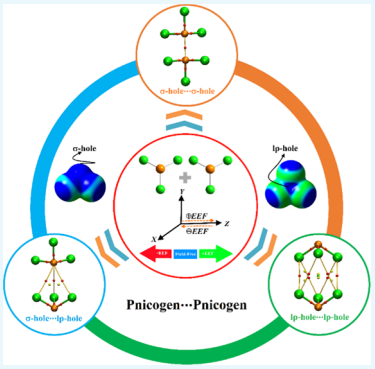

1. INTRODUCTION

Noncovalent interactions have recently been the subject of many studies due to the recognition of their key role in drug discovery,[1−3] crystal engineering,[4,5] and materials science.[6−8] Among noncovalent interactions, hole bonds have recently evoked an exceptional interest. In a series of studies, the covalently bonded atoms of group IV−VII were reported with recognizable ability to form regions of depletion in electron density,[9−12] dubbed as σ-,[13] π-,[14] lone-pair (lp)-,[15] and radical ($R^{\bullet}$)-holes.[16] The holes of group IV−VII element-containing molecules can interact with Lewis bases, forming tetrel,[17−19] pnicogen,[20−25] chalcogen,[26−31] and halogen[13,31−36] bonds, respectively. Among hole-bonding complexes, the interactions of pnicogen-containing molecules with Lewis bases have found sustained attention of a variety of theoretical[37−42] and experimental studies[43−45] by dint of their significant importance in chemical reactions[46−48] and biological systems.[49]

More recently, like···like noncovalent interactions have triggered a rich trove of interest because of their genuine roles in material and crystal design.[50−53] In that spirit, many studies have recently been established to elucidate the features of like···like noncovalent interactions, in which the intermolecular interaction occurred between two similar atoms within the like···like configuration. The interactions involving the covalently bonded halogen atoms represent the most well-known type of like···like interactions.[54−60] Parallel to halogen···halogen interactions, the interactions of chalcogens,[61,62] tetrels,[63−65] and triels[66] within like···like configurations were thoroughly addressed. However, a great deal of interest has been directed toward the investigation of pnicogen bonds; there is a paucity in the literature pertinent to the pnicogen···pnicogen interactions.

One of the most crucial factors that affect noncovalent interactions is the external electric field (EEF). As a point of departure, Bandrauk et al. elucidated the effect of the intense local electric fields (ranging from ∼10^8 to ∼10^{10} V/m) arising from the surrounding medium of the biological systems.[67,68] Subsequently, a flurry of studies has been devoted to illustrating the EEF effect on variant noncovalent interac-

Received: January 10, 2022
Accepted: March 11, 2022
Published: March 22, 2022

https://doi.org/10.1021/acsomega.2c00176
ACS Omega 2022, 7, 11264−11275

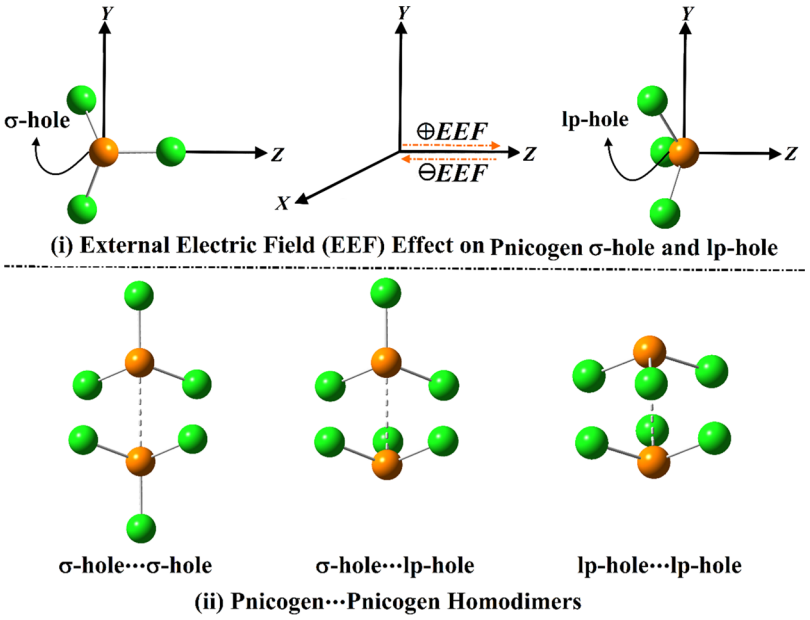

Figure 1. Representation of (i) EEF effect on pnicogen σ-hole and lone-pair (lp)-hole and (ii) pnicogen···pnicogen homodimers within σ-hole···σ-hole, σ-hole···lp-hole, and lp-hole···lp-hole configurations. The positive and negative signs represent the directionality of the employed EEF.

tions.[69−72] Upon careful literature review, the EEF has demonstrated exceptional influence on the strength of the noncovalently bonded complexes. Nevertheless, there is a paucity in the literature relevant to its effect on versatile σ-hole and lp-hole interactions, in particular, within pnicogen-bearing complexes.

Accordingly, the current study was devoted to thoroughly elucidate the features of the σ-hole and lp-hole interactions of pnicogen···pnicogen homodimers $(PCl_3)_2$ within σ-hole···σ-hole, σ-hole···lp-hole, and lp-hole···lp-hole configurations, for the first time, under field-free conditions and the influence of an EEF (Figure 1). The employed EEF strengths were set to be 0.002, 0.004, and 0.008 au, which suited in the range of the electric field within the biological systems (i.e., 0.0002−0.0194 au). Versatile quantum mechanical calculations, including geometrical optimization, molecular electrostatic potential (MEP) maps, and surface electrostatic potential extrema ($V_{s,max}$), were carried out for the investigated PCl_3 molecules under field-free and directed EEF conditions. Besides, the point-of-charge (PoC) approach was executed as an indicative tool for the electrostatic potentiality of the studied systems to attractively interact with Lewis bases and acids within a small scale (using PoC with values of −0.50 and +0.50 au, respectively). For pnicogen···pnicogen homodimers, the energetic quantities were thoroughly assessed using MP2 and CCSD/CBS levels of theory. Toward an in-depth insight, the quantum theory of atoms in molecules (QTAIM) and the noncovalent interaction (NCI) index were adopted to clarify the nature of the selected interactions from a topological perspective. The given results are not only substantial for the central understanding of pnicogen···pnicogen homodimers as essential molecular linkers but also informative for near-future technological applications pertinent to EEF.

2. COMPUTATIONAL METHODS

The versatility of the pnicogen-bearing monomers PCl_3 to engage in σ-hole and lp-hole interactions of pnicogen··· pnicogen homodimers within σ-hole···σ-hole, σ-hole···lp-hole, and lp-hole···lp-hole configurations was comparatively scrutinized (Figure 1). The studied monomers and homodimers were first optimized under field-free conditions and the influence of EEF by the second-order Møller−Plesset perturbation theory (MP2) method[73] with the aug-cc-pVTZ basis set.[74−76] In geometry optimization of homodimers, no symmetry restrictions were considered. The utilized EEF was directed along the z-axis in both positive and negative directions, with values ranging from 0.002, 0.004, to 0.008 au (Figure 1). No vibrational frequency calculations were carried out for the optimized complexes, which gave rise to the possibility that the structures were not energetic minima. Upon the optimized monomers, the MEP maps were generated to visualize the electrophilic and nucleophilic sites on the surfaces of the chemical systems. Also, the $V_{s,max}$ at the σ-hole and lp-hole over the surface of the optimized PCl_3 monomers were assessed with the help of the Multiwfn 3.7 package[77] using a 0.002 au electron density contour based on earlier recommendations.[54,78]

With the help of the PoC approach, an electrostatic model for pnicogen-based interactions was investigated, for the first time, under field-free conditions and the influence of the negatively and positively directed EEF. In the context of the PoC approach, the negatively and positively charged points were utilized with a value of ±0.50 au to mimic the roles of Lewis bases and acids,[16,33,79,80] respectively. Besides, the P··· PoC distance effect was thoroughly studied in the range of 2.5−6.0 Å with a step size of 0.1 Å. Molecular stabilization energy ($E_{stabilization}$) was then computed according to the following equation[15,81]

$$E_{stabilization} = E_{pnicogen-containing\ molecule\cdots PoC} - E_{pnicogen-containing\ molecule} \quad (1)$$

For the optimized homodimers, interaction energies were calculated under field-free conditions and the influence of the negatively and positively directed EEF, as the difference in energy between the complex and the sum of the monomers at

https://doi.org/10.1021/acsomega.2c00176
ACS Omega 2022, 7, 11264−11275

the MP2/aug-cc-pVTZ level of theory. The interaction energies were then benchmarked at the CCSD(T)/CBS level and calculated as follows[82]

$$E_{\mathrm{CCSD(T)/CBS}} = \Delta E_{\mathrm{MP2/CBS}} + \Delta E_{\mathrm{CCSD(T)}} \quad (2)$$

where

$$\Delta E_{\mathrm{MP2/CBS}} = (64E_{\mathrm{MP2/aug-cc-pVQZ}} - 27E_{\mathrm{MP2/aug-cc-pVTZ}})/37 \quad (3)$$

$$\Delta E_{\mathrm{CCSD(T)}} = E_{\mathrm{CCSD(T)/aug-cc-pVDZ}} - E_{\mathrm{MP2/aug-cc-pVDZ}} \quad (4)$$

The basis set superposition error (BSSE) was eliminated from the computed MP2 and CCSD(T) energetic quantities by incorporating the counterpoise correction (CC) procedure.[83] To elucidate the topological features of the studied interactions, QTAIM[84] was invoked. Using QTAIM, bond critical points (BCPs) and bond paths (BPs) were generated. Furthermore, the electron density (ρ_b) and Laplacian ($\nabla^2\rho_b$) were evaluated. The noncovalent interaction (NCI) index was also adopted to investigate the origin of the σ-hole and lp-hole interactions within the investigated pnicogen···pnicogen homodimers based on the electron density and its derivatives.[85] QTAIM and NCI index analyses were performed using Multiwfn 3.7 software,[77] and their plots were graphed with Visual Molecular Dynamics (VMD) software.[86] All the remaining quantum mechanical calculations were carried out using Gaussian09 software.[87]

Furthermore, symmetry-adapted perturbation theory-based energy decomposition analysis (SAPT-EDA) was executed to elucidate the physical nature of the studied interactions. In that spirit, the physical energetic components, involving electrostatic (E_{elst}), induction (E_{ind}), dispersion (E_{disp}), and exchange (E_{exch}), were assessed for the investigated homodimers with the help of the PSI4 code[88] at the SAPT2 level of truncation[89] using the aug-cc-PVTZ basis set. The total SAPT2 energy (E_{SAPT2}) could be given according to the following equations[90]

$$E_{\mathrm{SAPT2}} = E_{\mathrm{elst}} + E_{\mathrm{ind}} + E_{\mathrm{disp}} + E_{\mathrm{exch}} \quad (5)$$

where

$$E_{\mathrm{elst}} = E_{\mathrm{elst}}^{(10)} + E_{\mathrm{elstr}}^{(12)} \quad (6)$$

$$E_{\mathrm{ind}} = E_{\mathrm{indr}}^{(20)} + E_{\mathrm{exch-indr}}^{(20)} + E_{\mathrm{ind}}^{(22)} + E_{\mathrm{exch-ind}}^{(22)} + \delta E_{\mathrm{HFr}}^{(2)} \quad (7)$$

$$E_{\mathrm{disp}} = E_{\mathrm{disp}}^{(20)} + E_{\mathrm{exch-disp}}^{(20)} \quad (8)$$

$$E_{\mathrm{exch}} = E_{\mathrm{exch}}^{(10)} + E_{\mathrm{exch}}^{(11)} + E_{\mathrm{exch}}^{(12)} \quad (9)$$

3. RESULTS AND DISCUSSION

3.1. MEP Calculations. MEP maps have been considered as a real descriptor for the charge distribution along the molecular surfaces of the noncovalent bond donors and acceptors.[91−93] Whereby MEP maps, low and high electron densities are identified by the colored maps, where blue and red sites are prone to nucleophilic and electrophilic attacks, respectively. In the current study, MEP maps were generated under field-free conditions and the effect of EEF using 0.002 au electron density contour. Further quantitative evidence was introduced by evaluating $V_{s,max}$ at the σ-hole and lp-hole over the surface of the optimized PCl_3 monomer (Figure 2). The MEP maps along with $V_{s,max}$ values under the influence of the

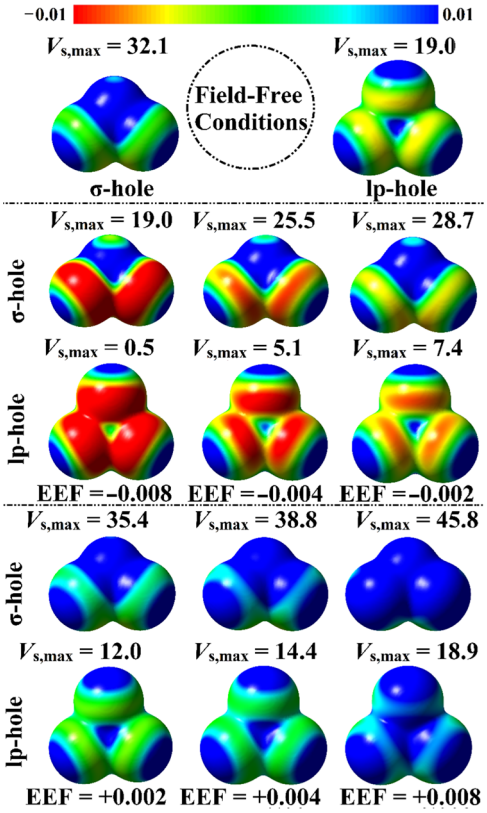

Figure 2. MEP maps for PCl_3 molecules as σ-hole and lp-hole under field-free conditions and the influence of the negatively and positively directed EEF with values ranging from 0.002 to 0.008 au. The electrostatic potential varies from −0.01 (red) to +0.01 (blue) au. The surface electrostatic potential extrema ($V_{s,max}$) are computed (in kcal/mol) at the σ-hole and lp-hole of the phosphorous atom.

EEF are illustrated in Figure 2. The correlation of the EEF strength and direction with the $V_{s,max}$ values at the σ-hole and lp-hole of the optimized PCl_3 monomer is displayed in Figure 3.

Looking at Figure 2, the occurrence of pnicogen σ-hole and lp-hole on the surface of the investigated PCl_3 molecules was obviously noticed. The prominent size of the blue region was detected in the case of σ-hole, outlining the further favorability of phosphorous, as a pnicogen bond donor, to interact via σ-hole rather than lp-hole. By applying EEF, as illustrated in Figure 2, the sizes of σ-holes and lp-holes were increased and decreased by orienting the employed EEF in the positive and negative directions, respectively. In the same context, the data shown in Figure 3 consistently revealed the direct and reverse correlation between the positive value of the $V_{s,max}$ and the strength of the negatively and positively directed EEF, respectively.

3.2. PoC Calculations. In the PoC approach, negatively and positively charged points are utilized to mimic the role of Lewis bases and acids in noncovalent interactions. The nucleophilic and electrophilic natures of the chemical systems are accordingly addressed from an electrostatic perspective in terms of molecular stabilization energy.[33] The PoC approach has recently been notarized as a trustworthy method for studying the σ-hole,[94−96] lp-hole,[15] π-hole,[97,98] and $R^{\bullet}$-hole[99]

https://doi.org/10.1021/acsomega.2c00176
ACS Omega 2022, 7, 11264−11275

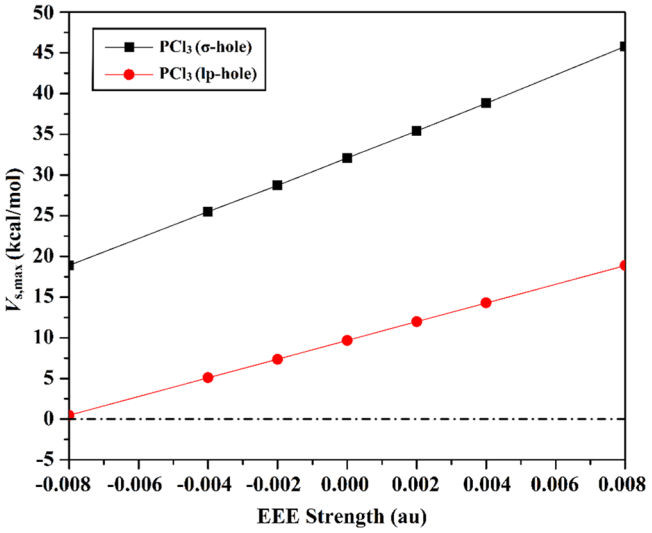

Figure 3. Correlation between the EEF strength and the surface electrostatic potential extrema ($V_{s,max}$). The EEF's positive and negative charges were adopted to illustrate the positive and negative directions, respectively.

interactions from an electrostatic point of view.[15,99,100] With the help of the PoC approach, the ability of the PCl_3 molecule to interact with Lewis bases and acids was investigated by employing negative and positive PoCs, respectively. $^{\pm}\sigma$-Hole and $^{\pm}$lp-hole tests were executed for the optimized PCl_3 molecule under the influence of 0.000, ±0.002, ±0.004, ± 0.006, and ±0.008 au EEF at σ-hole··· and lp-hole···PoC distance in the range of 2.5−6.0 Å with a step size of 0.1 Å using a PoC value of ±0.50 au. Molecular stabilization energy curves were generated and are displayed in Figure 4. Table 1 gathers molecular stabilization energies of the σ-hole··· and lp-hole···PoC systems at a distance of 2.5 Å.

For $^{-}\sigma$-hole and $^{-}$lp-hole tests, it was noticed from the data in Figure 4 that the optimized PCl_3···PoC systems exhibited the most significant negative molecular stabilization energies in the presence of the positively directed EEF, followed by the absence of EEF, and finally the negatively directed EEF. From Table 1, as an illustration, the molecular stabilization energies of the σ-hole···PoC electrostatic model were found with values of −10.84, −11.85, and −9.71 kcal/mol under the influence of 0.000, +0.002, and −0.002 au EEF, respectively.

With regard to the effect of the EEF strength, the molecular stabilization energy increased with increasing the magnitude of

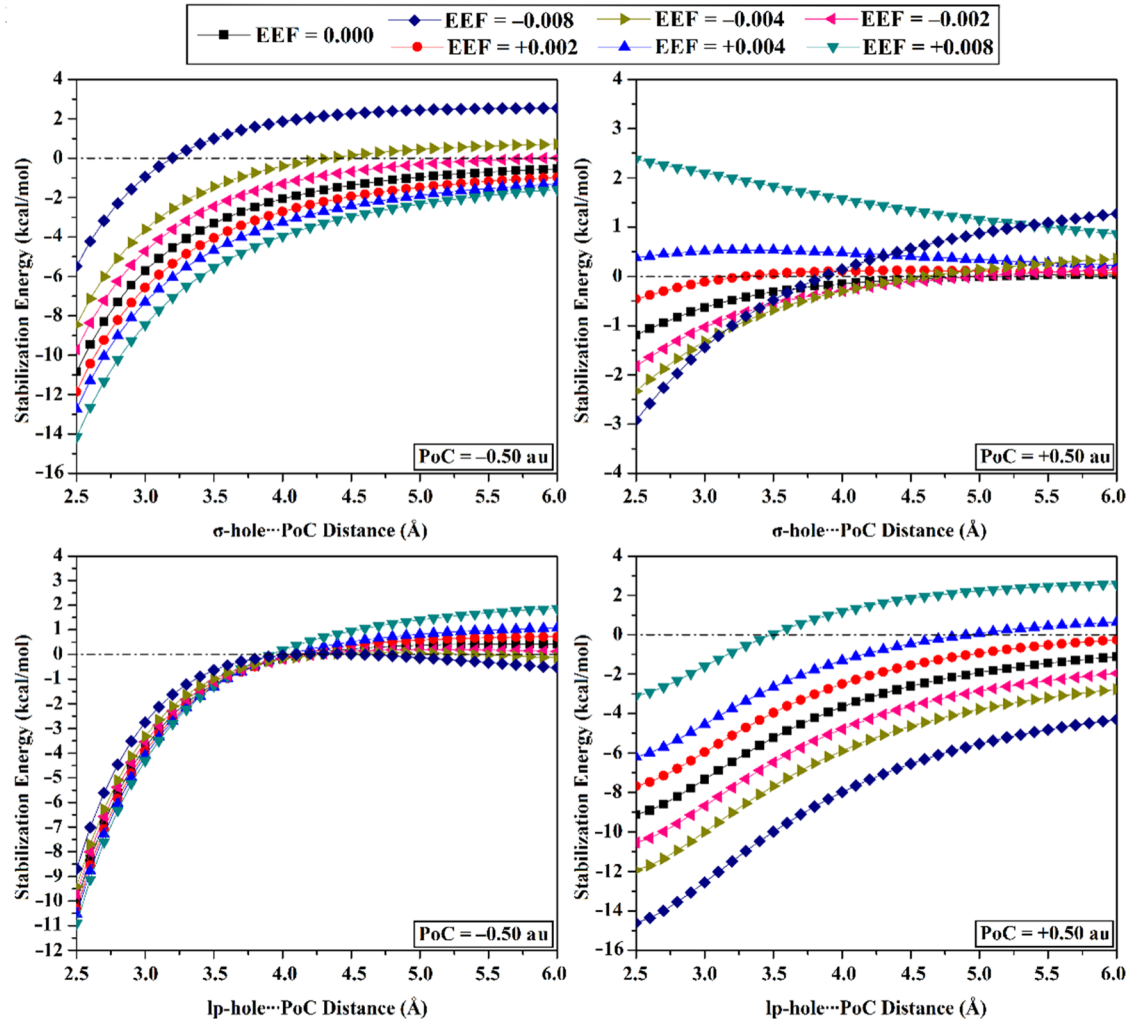

Figure 4. Molecular stabilization energy curves for the PCl_3···PoC systems calculated at σ-hole··· and lp-hole···PoC distance in the range of 2.5−6.0 Å under the field-free condition and the influence of the negatively and positively directed EEF with values ranging from 0.002 to 0.008 au in the presence of ±0.50 au PoC.

https://doi.org/10.1021/acsomega.2c00176
ACS Omega 2022, 7, 11264−11275

Table 1. Molecular Stabilization Energy ($E_{stabilization}$) Values for the PCl_3···PoC Systems Calculated at a σ-Hole··· and lp-Hole···PoC Distance of 2.5 Å under the Field-Free Condition and the Influence of the Negatively and Positively Directed EEF with Values Ranging from 0.002 to 0.008 au in the Presence of ±0.50 au PoC

		molecular stabilization energy ($E_{stabilization}$, kcal/mol)	
PCl_3···PoC	EEF (au)	−0.50	+0.50
σ-hole···PoC	−0.008	−5.49	−2.92
	−0.004	−8.46	−2.33
	−0.002	−9.71	−1.82
	0.000	−10.84	−1.19
	+0.002	−11.85	−0.46
	+0.004	−12.74	0.38
	+0.008	−14.15	2.38
lp-hole···PoC	−0.008	−8.69	−14.61
	−0.004	−9.41	−11.93
	−0.002	−9.73	−10.54
	0.000	−10.03	−9.12
	+0.002	−10.29	−7.67
	+0.004	−10.53	−6.19
	+0.008	−10.91	−3.11

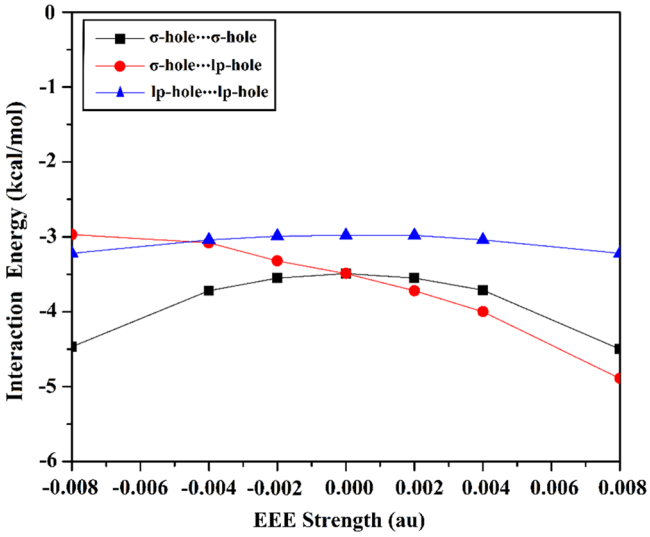

Figure 5. Interaction energy of the $(PCl_3)_2$ homodimers within σ-hole···σ-hole, σ-hole···lp-hole, and lp-hole···lp-hole configurations computed (in kcal/mol) at the MP2/aug-cc-pVTZ level of theory under the field-free condition and the influence of the negatively and positively directed EEF with values ranging from 0.002 to 0.008 au.

the positively directed EEF value and decreased by applying the EEF along the reverse direction. For instance, in the case of σ-hole interactions, the molecular stabilization energies of the PCl_3···PoC systems exhibited values of −11.85, −12.74, and −14.15 kcal/mol under the influence of +0.002, +0.004, and +0.008 au EEF, respectively. Conspicuously, the highly appreciated electrostatic interactions of the PCl_3···PoC systems were observed by the occurrence of the substantial negative molecular stabilization energies in the case of σ-hole···PoC more than that of lp-hole···PoC.

Turning to the results of $^{+}$σ-hole, it can be seen from the data in Figure 4 that the molecular stabilization energies were progressively faded, and then the molecular destabilization energies boosted by applying the EEF along the positive direction. In contrast, the negatively directed EEF enhanced the strength of the PCl_3···PoC systems.

In the presence of the +0.50 au PoC, the lp-hole electrostatic interactions exhibited the most considerable molecular stabilization energies, particularly under the influence of the −0.008 au EEF with a value of −14.61 kcal/mol. Such significant energies outlined the prominent contributions of the three coplanar atoms in the strength of lp-hole-based interactions. In all instances, the strength of the positively directed EEF exhibited direct and reversed correlations with the molecular stabilization energies of the PCl_3···PoC systems in the presence of negative and positive PoC, respectively. The reversed pattern was detected for the strength of the negatively directed EEF.

3.3. Energetic Study. σ-Hole and lp-hole interactions of the $(PCl_3)_2$ homodimers were comparatively studied within the σ-hole···σ-hole, σ-hole···lp-hole, and lp-hole···lp-hole configurations (see Figure 1). Geometrical optimization was first performed at the MP2/aug-cc-pVTZ level of theory for the investigated homodimers under the field-free condition and the influence of the negatively and positively directed EEF. Upon the optimized homodimers, interaction energies were computed at the same level of theory and are correlated with the EEF strength and direction in Figure 5.

As shown in Figure 5, all the considered homodimers demonstrated potent potentiality to participate in pnicogen σ-hole and lp-hole interactions within the σ-hole···σ-hole, σ-hole···lp-hole, and lp-hole···lp-hole configurations. The superior negative interaction energies were ascribed to the $(PCl_3)_2$ homodimers within the σ-hole···lp-hole configuration, followed by σ-hole···σ-hole and lp-hole···lp-hole configurations. From Table 2, it can be seen that the interaction energies were −3.72, −3.55, and −2.98 kcal/mol for the $(PCl_3)_2$ homodimers within σ-hole···lp-hole, σ-hole···σ-hole, and lp-hole···lp-hole configurations, respectively, under the influence of +0.002 au EEF.

For σ-hole···σ-hole and lp-hole···lp-hole configurations, the directionality effect of the employed EEF nearly vanished, which might be interpreted as a consequence of their symmetrical nature. The enhancement of the interaction energy of the $(PCl_3)_2$ homodimers was detected by increasing the strength of the employed EEF. For example, the interaction energies showed values of −3.55, −3.71, and −4.50 kcal/mol for the optimized $(PCl_3)_2$ homodimers within the σ-hole···σ-hole configuration under the influence of ±0.002, ±0.004, and ±0.008 au EEF, respectively.

On the other hand, for an antisymmetric σ-hole···lp-hole configuration, it was observed that the interaction energies of the inspected homodimers increased and decreased by applying EEF along the positive and negative directions, respectively. The interaction energies exhibited a direct and an inverse correlation with the strength of the adopted EEF along positive and negative directions, respectively. Also, the intermolecular distances within the studied homodimers were noticed to be inversely and directly correlated with the strength of the negatively and positively directed EEF. Numerically, the intermolecular distances of the optimized $(PCl_3)_2$ homodimers within the σ-hole···lp-hole configuration under the influence of +0.008, +0.004, and +0.002 au EEF were 4.00, 4.03, and 4.08 Å, respectively.

Moreover, the benchmarking of the interaction energies was carried out for all the examined homodimers at the MP2/CBS

https://doi.org/10.1021/acsomega.2c00176
ACS Omega 2022, 7, 11264−11275

Table 2. Interaction Energies Calculated (in kcal/mol) at MP2/aug-cc-pVTZ, MP2/CBS, and CCSD(T)/CBS Levels of Theory of the $(PCl_3)_2$ Optimized Homodimers under the Field-Free Condition and the Influence of the Negatively and Positively Directed EEF with Values Ranging from 0.002 to 0.008 au

			$E_{MP2/aug\text{-}cc\text{-}pVTZ}$ (kcal/mol)				
configuration	EEF (au)	distance[a] (Å)	BSSE-uncorrected	BSSE-corrected	estimated BSSE	$E_{MP2/CBS}$ (kcal/mol)	$E_{CCSD(T)}$/CBS (kcal/mol)
σ-hole···σ-hole	−0.008	3.08	−6.25	−4.47	0.0028	−5.47	−3.50
	−0.004	3.15	−5.41	−3.72	0.0027	−4.58	−2.84
	−0.002	3.17	−5.21	−3.55	0.0026	−4.38	−2.71
	0.000	3.16	−5.16	−3.49	0.0026	−4.34	−2.66
	+0.002	3.16	−5.22	−3.55	0.0027	−4.40	−2.71
	+0.004	3.15	−5.39	−3.71	0.0027	−4.57	−2.84
	+0.008	3.08	−6.25	−4.50	0.0028	−5.50	−3.52
σ-hole···lp-hole	−0.008	4.59	−3.97	−2.97	0.0016	−3.54	−2.51
	−0.004	4.41	−4.18	−3.08	0.0017	−3.69	−2.60
	−0.002	4.13	−4.58	−3.32	0.0020	−3.98	−2.78
	0.000	4.10	−4.79	−3.49	0.0021	−4.16	−2.92
	+0.002	4.08	−5.06	−3.72	0.0021	−4.43	−3.15
	+0.004	4.03	−5.40	−4.00	0.0022	−4.78	−3.41
	+0.008	4.00	−6.36	−4.89	0.0023	−5.74	−4.26
lp-hole···lp-hole	−0.008	5.23	−4.13	−3.22	0.0015	−3.86	−2.78
	−0.004	5.23	−3.93	−3.04	0.0014	−3.66	−2.58
	−0.002	5.23	−3.88	−2.99	0.0014	−3.61	−2.54
	0.000	5.23	−3.87	−2.98	0.0014	−3.59	−2.52
	+0.002	5.23	−3.88	−2.98	0.0014	−3.60	−2.52
	+0.004	5.23	−3.93	−3.04	0.0014	−3.65	−2.57
	+0.008	5.23	−4.13	−3.22	0.0014	−3.86	−2.78

[a]Distances between the two interacted phosphorous atoms of the pnicogen homodimers within the modeled σ-hole···σ-hole, σ-hole···lp-hole, and lp-hole···lp-hole configurations.

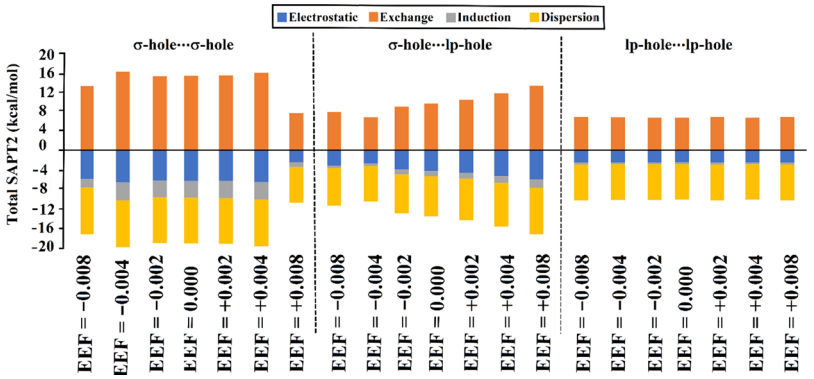

Figure 6. Bar chart for physical components of total SAPT2 energy including electrostatic (E_{elst}), induction (E_{ind}), dispersion (E_{disp}), and exchange (E_{exch}) components for pnicogen···pnicogen $(PCl_3)_2$ homodimers under the field-free condition and the effect of negatively and positively directed EEF.

and CCSD/CBS levels of theory. The computed MP2/CBS and CCSD(T)/CBS interaction energies are compiled in Table 2, revealing a near similarity between the interaction energy values computed at both levels of theory. Besides, the effect of the directed EEF on the BSSE-CC was evaluated (Table 2). According to the data listed in Table 2, the EEF demonstrated a negligible effect on the computed BSSE values. Toward further accuracy, the effect of consideration of BSSE-CC in geometry optimization was examined for the $(PCl_3)_2$ homodimer within the three studied configurations. The examined homodimers were optimized with and without BSSE-CC, and the corresponding interaction energies were computed. According to the results, the difference between the interaction energies of the BSSE-corrected and BSSE-uncorrected optimized geometries were −0.08, −0.10, and −0.05 kcal/mol for σ-hole···σ-hole, σ-hole···lp-hole, and lp-hole···lp-hole configurations, respectively. Consequently, the obtained results affirmed that the consideration of BSSE-CC in the geometry optimization had a negligible effect on the computed interaction energies.

3.4. SAPT-EDA Calculations. The symmetry-adapted perturbation theory-based energy decomposition analysis (SAPT-EDA) has been confirmed as an informative tool for determining the physical nature of noncovalent interactions.[101,102] In the context of SAPT-EDA, the total interaction energy is directly decomposed into its four physical meaningful components, including electrostatic (E_{elst}), exchange (E_{exch}), induction (E_{ind}), and dispersion (E_{disp}) forces (Figure 6). For optimized homodimers, SAPT-EDA was carried out at the SAPT2 level of truncation using the PSI4 code,[88] and the released components are collected in Table 3.

https://doi.org/10.1021/acsomega.2c00176
ACS Omega 2022, 7, 11264−11275

Table 3. Electrostatic (E_{elst}), Induction (E_{ind}), Dispersion (E_{disp}), and Exchange (E_{exch}) Energies of the Optimized $(PCl_3)_2$ Homodimers Calculated in kcal/mol at the SAPT2 Level of Truncation under the Field-Free Condition and the Influence of the Negatively and Positively Directed EEF with Values Ranging from 0.002 to 0.008 au

configuration	EEF (au)	E_{elst} (kcal/mol)	E_{ind} (kcal/mol)	E_{disp} (kcal/mol)	E_{exch} (kcal/mol)	$E_{Total\ SAPT2}$ (kcal/mol)
σ-hole···σ-hole	−0.008	−8.04	−4.53	−10.63	19.47	−3.73
	−0.004	−6.64	−3.67	−9.68	16.24	−3.75
	−0.002	−6.24	−3.44	−9.40	15.32	−3.76
	0.000	−6.28	−3.46	−9.42	15.41	−3.75
	+0.002	−6.32	−3.48	−9.45	15.50	−3.76
	+0.004	−6.54	−3.61	−9.62	16.03	−3.75
	+0.008	−8.11	−4.56	−10.61	19.55	−3.73
σ-hole···lp-hole	−0.008	−2.44	−0.44	−6.89	6.36	−3.41
	−0.004	−2.67	−0.55	−7.31	6.86	−3.67
	−0.002	−3.95	−1.00	−8.00	9.01	−3.93
	0.000	−4.27	−1.10	−8.25	9.67	−3.94
	+0.002	−4.63	−1.23	−8.51	10.43	−3.94
	+0.004	−5.25	−1.44	−9.01	11.77	−3.92
	+0.008	−5.98	−1.73	−9.58	13.37	−3.92
lp-hole···lp-hole	−0.008	−2.54	−0.36	−7.42	6.92	−3.40
	−0.004	−2.49	−0.35	−7.35	6.79	−3.40
	−0.002	−2.49	−0.35	−7.35	6.78	−3.40
	0.000	−2.48	−0.35	−7.33	6.75	−3.40
	+0.002	−2.53	−0.35	−7.39	6.88	−3.40
	+0.004	−2.49	−0.35	−7.34	6.78	−3.40
	+0.008	−2.54	−0.36	−7.41	6.91	−3.40

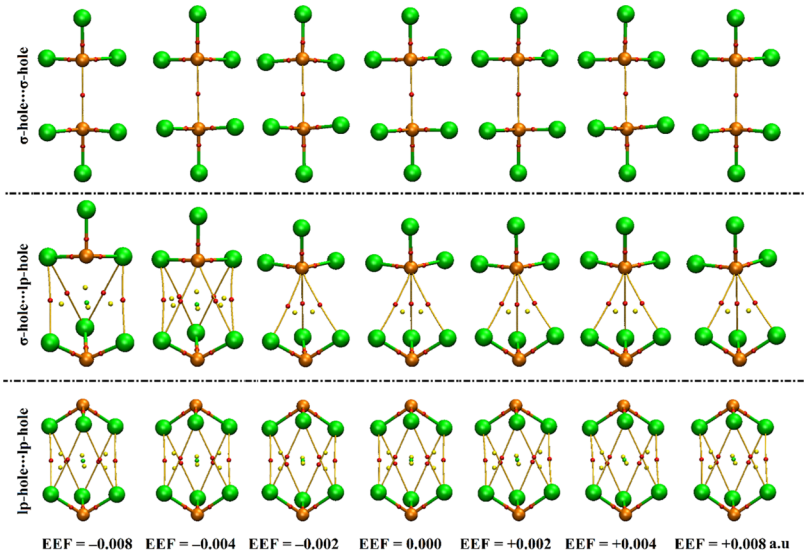

Figure 7. QTAIM diagrams for the optimized $(PCl_3)_2$ homodimers under the field-free condition and the influence of the negatively and positively directed EEF with values ranging from 0.002 to 0.008 au. Red dots represent the location of BCPs and BPs.

From the data registered in Table 3, it can be seen that the studied interactions within all the inspected $(PCl_3)_2$ homodimers were dominated by the dispersion energy (E_{disp}), which were earlier reported in the case of halogen, chalcogen, and tetrel homodimers.[62,65,100] Besides, obvious contributions for the electrostatic (E_{elst}) and induction (E_{ind}) interactions were also recognized in the designed pnicogen σ-hole and lp-hole interactions. However, exchange energy (E_{exch}) demonstrated positive values for all homodimers, outlining unfavorable exchange contributions to the strength of the explored interactions (Figure 6). As an illustration, in the case of σ-hole···σ-hole homodimer under the field-free condition, the E_{elst}, E_{ind}, E_{disp}, and E_{exch} values were −6.28, −3.46, −9.42, and 15.41 kcal/mol, respectively (Table 3).

Consistent with the energetic findings listed in Table 2, the utilization of the EEF generally increased the contributions of the E_{elst}, E_{ind}, and E_{disp} components for all the studied homodimers. For instance, the E_{disp} values of the homodimers within the σ-hole···lp-hole interactions were −8.25, −8.51, −9.01, and −9.58 kcal/mol under the influence of 0.000, +0.002, +0.004, and +0.008 au EEF strength, respectively.

In line with the MP2 results, the most prominent negative total SAPT2 energy was noticed in the case of σ-hole···lp-hole configuration, followed by σ-hole···σ-hole and lp-hole···lp-hole configurations. For instance, the total SAPT2 energies were −3.94, −3.76, and −3.40 kcal/mol for the $(PCl_3)_2$ homodimers within σ-hole···lp-hole, σ-hole···σ-hole, and lp-hole···lp-

https://doi.org/10.1021/acsomega.2c00176
ACS Omega 2022, 7, 11264−11275

hole configurations, respectively, under the influence of +0.002 au EEF.

3.5. QTAIM Analysis. QTAIM has been documented as an intuitive technique that probes the nature of noncovalent interactions.[103−106] Using QTAIM, the BPs and the (3,−1) BCPs were generated to provide qualitative clues for the occurrence of σ-hole and lp-hole interactions (Figure 7). Furthermore, the topological features, including electron density (ρ_b) and Laplacian ($\nabla^2\rho_b$), were calculated and are collected in Table 4.

Table 4. Electron Density (ρ_b, au) and Laplacian ($\nabla^2\rho_b$, au) at BCPs of the Optimized $(PCl_3)_2$ Homodimers under the Field-Free Condition and the Influence of the Negatively and Positively Directed EEF with Values Ranging from 0.002 to 0.008 au

configuration	EEF	ρ_b (au)	$\nabla^2\rho_b$ (au)
σ-hole···σ-hole	−0.008	0.0222	0.0354
	−0.004	0.0194	0.0343
	−0.002	0.0186	0.0338
	0.000	0.0187	0.0339
	+0.002	0.0188	0.0339
	+0.004	0.0192	0.0342
	+0.008	0.0223	0.0354
σ-hole···lp-hole	−0.008	0.0053	0.0177
	−0.004	0.0048	0.0163
	−0.002	0.0080	0.0247
	0.000	0.0087	0.0262
	+0.002	0.0095	0.0280
	+0.004	0.0071	0.0210
	+0.008	0.0078	0.0232
lp-hole···lp-hole	−0.008	0.0046	0.0155
	−0.004	0.0046	0.0156
	−0.002	0.0045	0.0150
	0.000	0.0045	0.0150
	+0.002	0.0047	0.0160
	+0.004	0.0047	0.0160
	+0.008	0.0049	0.0164

As displayed in Figure 7, all the studied homodimers were observed with variant numbers of BCPs and BPs that differ based on the configuration of the interacting species. Conspicuously, one, three, four, and six BCPs and BPs were noticed for the $(PCl_3)_2$ homodimers within the σ-hole···σ-hole, σ-hole···lp-hole, and lp-hole···lp-hole configurations, confirming the prominent contributions of the three coplanar atoms to the strength of the lp-hole based interactions. From Table 4, the closed shell nature of the σ-hole and lp-hole interactions within the considered homodimers was revealed by the relatively low values of ρ_b and the positive values of $\nabla^2\rho_b$.

Similar to energetic results, the ρ_b and $\nabla^2\rho_b$ values were decreased and increased by employing the negatively and positively directed EEF, respectively. For example, the ρ_b values of the optimized $(PCl_3)_2$ homodimers within the σ-hole···lp-hole configuration under −0.002, 0.000, and +0.002 au EEF were 0.0080, 0.0087, and 0.0095 au, respectively.

3.6. NCI Analysis. Noncovalent interaction (NCI) index[85,107] was herein invoked to precisely illustrate the nature and origin of the examined intermolecular interactions based on the electron density and its derivatives. Within the context of the NCI index, 3D NCI plots were generated with a reduced density gradient (RDG) value of 0.50 au and are displayed for all the studied homodimers in Figure 8.

As shown in Figure 8, green regions were observed for all the considered complexes, ensuring the occurrence of attractive forces between the two interacting species. Obviously, the size of the green regions exhibited the same pattern as the energetic quantities (Table 2). For example, the green-coded spheres of the interactions within the σ-hole···σ-hole and lp-hole···lp-hole configurations enlarged by increasing the magnitude of EEF in both positive and negative directions in the order 0.002 < 0.004 < 0.008 au. Also, the largest green-coded spheres were noticed in the case of $(PCl_3)_2$ homodimers within the σ-hole··· lp-hole configuration, followed by σ-hole···σ-hole and lp-hole··· lp-hole configurations that were in great consistency with the energetic affirmations and QTAIM observations. Overall, the findings of the QTAIM and NCI analyses remarkably confirmed the availability of $(PCl_3)_2$ homodimers to bond by

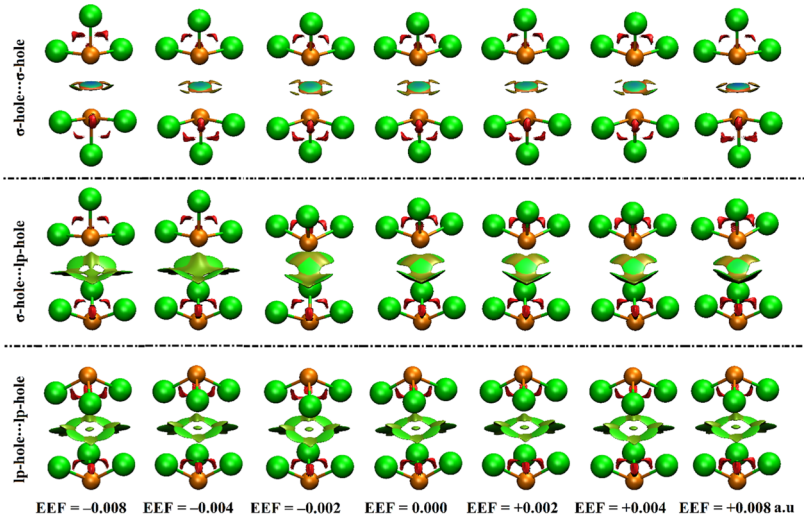

Figure 8. Noncovalent interaction (NCI) plots of the optimized $(PCl_3)_2$ homodimers under the field-free condition and the influence of the negatively and positively directed EEF with values ranging from 0.002 to 0.008 au. The isosurfaces are graphed with a RDG value of 0.50 au and colored according to sign(λ_2)ρ with a range from −0.035 (blue) to 0.020 (red) au.

https://doi.org/10.1021/acsomega.2c00176
ACS Omega 2022, 7, 11264−11275

σ-hole and lp-hole interactions within σ-hole···σ-hole, σ-hole··· lp-hole, and lp-hole···lp-hole configurations.

4. CONCLUSIONS

The potentiality of the σ-hole and lone-pair (lp)-hole pnicogen-containing molecules to form pnicogen···pnicogen homodimers $(PCl_3)_2$ within σ-hole···σ-hole, σ-hole···lp-hole, and lp-hole···lp-hole configurations was herein explored, for the first time, under field-free condition and the influence of the EEF. The following conclusions can be detected from MEP, $V_{s,max}$, PoC, interaction energy, SAPT-EDA, QTAIM, and NCI-based results: (i) the studied PCl_3 molecule has the ability to form σ-hole and lp-hole with higher tendency for the anterior one, (ii) the positively directed EEF enlarged the sizes of the pnicogen σ-hole and lp-hole, while the negatively directed EEF exhibited reverse amplitude, (iii) the investigated molecule more preferentially forms the pnicogen···pnicogen homodimer $(PCl_3)_2$ within the σ-hole···lp-hole configuration compared to the other modeled configurations, (iv) the strength of the studied homodimers within the σ-hole···lp-hole configuration boosted by directed EEF along the positive direction and plunged along the negative one, (v) the symmetrical nature of σ-hole···σ-hole and lp-hole···lp-hole configurations conclusively decline the directionality effect of the applied EEF, and finally (vi) the dispersion energy was announced as the most prevalent forces dominated the σ-hole and lp-hole interactions within the studied pnicogen··· pnicogen homodimers. These results would be informative for future research in the brain area of chemistry and materials science..

AUTHOR INFORMATION

Corresponding Author

Mahmoud A. A. Ibrahim − *Computational Chemistry Laboratory, Chemistry Department, Faculty of Science, Minia University, Minia 61519, Egypt;* orcid.org/0000-0003-4819-2040; Email: m.ibrahim@compchem.net

Authors

Nayra A. M. Moussa − *Computational Chemistry Laboratory, Chemistry Department, Faculty of Science, Minia University, Minia 61519, Egypt;* orcid.org/0000-0003-3712-7710

Sherif M. A. Saad − *Computational Chemistry Laboratory, Chemistry Department, Faculty of Science, Minia University, Minia 61519, Egypt*

Muhammad Naeem Ahmed − *Department of Chemistry, The University of Azad Jammu and Kashmir, Muzaffarabad 13100, Pakistan*

Ahmed M. Shawky − *Science and Technology Unit (STU), Umm Al-Qura University, Makkah 21955, Saudi Arabia*

Mahmoud E. S. Soliman − *Molecular Modelling and Drug Design Research Group, School of Health Sciences, University of KwaZulu-Natal, Durban 4000, South Africa;* orcid.org/0000-0002-8711-7783

Gamal A. H. Mekhemer − *Computational Chemistry Laboratory, Chemistry Department, Faculty of Science, Minia University, Minia 61519, Egypt*

Al-shimaa S. M. Rady − *Computational Chemistry Laboratory, Chemistry Department, Faculty of Science, Minia University, Minia 61519, Egypt*

Complete contact information is available at: https://pubs.acs.org/10.1021/acsomega.2c00176

Notes

The authors declare no competing financial interest.

ACKNOWLEDGMENTS

A.M.S. would like to thank the Deanship of Scientific Research at Umm Al-Qura University for supporting this work by Grant: 22UQU433174DSR03. The computational work was completed with resources supported by the Science and Technology Development Fund, STDF, Egypt, grant nos. 5480 and 7972.

REFERENCES

(1) Lu, Y.; Wang, Y.; Zhu, W. Nonbonding interactions of organic halogens in biological systems: Implications for drug discovery and biomolecular design. *Phys. Chem. Chem. Phys.* **2010**, *12*, 4543−4551.

(2) Lu, Y.; Liu, Y.; Xu, Z.; Li, H.; Liu, H.; Zhu, W. Halogen bonding for rational drug design and new drug discovery. *Expert Opin. Drug Discovery* **2012**, *7*, 375−383.

(3) Ibrahim, M. A. A.; Hasb, A. A. M.; Mekhemer, G. A. H. Role and nature of halogen bonding in inhibitor···receptor complexes for drug discovery: casein kinase-2 (CK2) inhibition as a case study. *Theor. Chem. Acc.* **2018**, *137*, 38−47.

(4) Braga, D.; Grepioni, F. Intermolecular interactions in nonorganic crystal engineering. *Acc. Chem. Res.* **2000**, *33*, 601−608.

(5) Robinson, J. M. A.; Philp, D.; Harris, K. D. M.; Kariuki, B. M. Weak interactions in crystal engineering—understanding the recognition properties of the nitro group. *New J. Chem.* **2000**, *24*, 799−806.

(6) Guo, X.; Liao, Q.; Manley, E. F.; Wu, Z.; Wang, Y.; Wang, W.; Yang, T.; Shin, Y.-E.; Cheng, X.; Liang, Y.; Chen, L. X.; Baeg, K.-J.; Marks, T. J.; Guo, X. Materials design via optimized intramolecular noncovalent interactions for high-performance organic semiconductors. *Chem. Mater.* **2016**, *28*, 2449−2460.

(7) Mahadevi, A. S.; Sastry, G. N. Cation-pi interaction: its role and relevance in chemistry, biology, and material science. *Chem. Rev.* **2013**, *113*, 2100−2138.

(8) Wang, M.; Li, W.; Lu, F.; Ding, X. Theoretical study on the stability of the complexes A...BX3 [A = CH3NH3(+), NH2CHNH2-(+), NH2CHOH(+); B = Sn(2+), Pb(2+); X = F(-), Cl(-), Br(-), I(-)]. *J. Mol. Model.* **2020**, *26*, 46.

(9) Alkorta, I.; Elguero, J.; Frontera, A. Not only hydrogen bonds: Other noncovalent interactions. *Crystals* **2020**, *10*, 180−208.

(10) Politzer, P.; Murray, J. S.; Clark, T. Halogen bonding and other σ-hole interactions: A perspective. *Phys. Chem. Chem. Phys.* **2013**, *15*, 11178−11189.

(11) Bauzá, A.; Mooibroek, T. J.; Frontera, A. The bright future of unconventional sigma/pi-hole interactions. *ChemPhysChem* **2015**, *16*, 2496−2517.

(12) Angarov, V.; Kozuch, S. On the σ, π and δ hole interactions: A molecular orbital overview. *New J. Chem.* **2018**, *42*, 1413−1422.

(13) Clark, T.; Hennemann, M.; Murray, J. S.; Politzer, P. Halogen bonding: the sigma-hole. Proceedings of "Modeling interactions in biomolecules II", Prague, September 5th-9th, 2005. *J. Mol. Model.* **2007**, *13*, 291−296.

(14) Murray, J. S.; Lane, P.; Clark, T.; Riley, K. E.; Politzer, P. Sigma-holes, pi-holes and electrostatically-driven interactions. *J. Mol. Model.* **2012**, *18*, 541−548.

(15) Ibrahim, M. A. A.; Telb, E. M. Z. A computational investigation of unconventional lone-pair hole interactions of group V−VIII elements. *ChemistrySelect* **2019**, *4*, 5489−5495.

(16) Ibrahim, M. A. A.; Telb, E. M. Z. Comparison of ±σ-hole and ±R̈-hole interactions formed by tetrel-containing complexes: A computational study. *RSC Adv.* **2021**, *11*, 4011−4021.

(17) Bauzá, A.; Mooibroek, T. J.; Frontera, A. Tetrel-bonding interaction: rediscovered supramolecular force? *Angew. Chem., Int. Ed.* **2013**, *52*, 12317−12321.

(18) Murray, J. S.; Lane, P.; Politzer, P. Expansion of the sigma-hole concept. *J. Mol. Model.* **2009**, *15*, 723−729.

(19) Grabowski, S. J. Tetrel bond-sigma-hole bond as a preliminary stage of the SN2 reaction. *Phys. Chem. Chem. Phys.* **2014**, *16*, 1824−1834.
(20) Li, Q.-Z.; Li, R.; Liu, X.-F.; Li, W.-Z.; Cheng, J.-B. Concerted interaction between pnicogen and halogen bonds in XCl-FH2P-NH3 (X=F, OH, CN, NC, and FCC). *ChemPhysChem* **2012**, *13*, 1205−1212.
(21) Scheiner, S. The pnicogen bond: its relation to hydrogen, halogen, and other noncovalent bonds. *Acc. Chem. Res.* **2013**, *46*, 280−288.
(22) Murray, J. S.; Lane, P.; Politzer, P. A predicted new type of directional noncovalent interaction. *Int. J. Quantum Chem.* **2007**, *107*, 2286−2292.
(23) Alkorta, I.; Elguero, J.; Del Bene, J. E. Pnicogen bonded complexes of PO2X (X = F, Cl) with nitrogen bases. *J. Phys. Chem. A* **2013**, *117*, 10497−10503.
(24) Bauzá, A.; Ramis, R.; Frontera, A. A combined theoretical and Cambridge Structural Database study of pi-hole pnicogen bonding complexes between electron rich molecules and both nitro compounds and inorganic bromides (YO2Br, Y = N, P, and As). *J. Phys. Chem. A* **2014**, *118*, 2827−2834.
(25) Bauzá, A.; Mooibroek, T. J.; Frontera, A. σ-Hole Opposite to a Lone Pair: Unconventional Pnicogen Bonding Interactions between ZF3(Z=N, P, As, and Sb) Compounds and Several Donors. *ChemPhysChem* **2016**, *17*, 1608−1614.
(26) Murray, J. S.; Lane, P.; Clark, T.; Politzer, P. σ-hole bonding: molecules containing group VI atoms. *J. Mol. Model.* **2007**, *13*, 1033−1038.
(27) Wang, W.; Ji, B.; Zhang, Y. Chalcogen bond: A sister noncovalent bond to halogen bond. *J. Phys. Chem. A* **2009**, *113*, 8132−8135.
(28) Adhikari, U.; Scheiner, S. Effects of charge and substituent on the S...N chalcogen bond. *J. Phys. Chem. A* **2014**, *118*, 3183−3192.
(29) Ibrahim, M. A. A.; Safy, M. E. A. A new insight for chalcogen bonding based on Point-of-Charge approach. *Phosphorus Sulfur Relat. Elem.* **2019**, *194*, 444−454.
(30) Esrafili, M. D.; Nurazar, R. Chalcogen bonds formed through π-holes: SO3 complexes with nitrogen and phosphorus bases. *Mol. Phys.* **2015**, *114*, 276−282.
(31) Aakeroy, C. B.; Bryce, D. L.; Desiraju, G. R.; Frontera, A.; Legon, A. C.; Nicotra, F.; Rissanen, K.; Scheiner, S.; Terraneo, G.; Metrangolo, P.; Resnati, G. Definition of the chalcogen bond (IUPAC Recommendations 2019). *Pure Appl. Chem.* **2019**, *91*, 1889−1892.
(32) Politzer, P.; Murray, J. S.; Clark, T. Halogen bonding: An electrostatically-driven highly directional noncovalent interaction. *Phys. Chem. Chem. Phys.* **2010**, *12*, 7748−7757.
(33) Ibrahim, M. A. A.; Hasb, A. A. M. Polarization plays the key role in halogen bonding: a point-of-charge-based quantum mechanical study. *Theor. Chem. Acc.* **2019**, *138*, 2−13.
(34) Wang, H.; Wang, W.; Jin, W. J. Sigma-hole bond vs pi-hole bond: A comparison based on halogen bond. *Chem. Rev.* **2016**, *116*, 5072−5104.
(35) Cavallo, G.; Metrangolo, P.; Milani, R.; Pilati, T.; Priimagi, A.; Resnati, G.; Terraneo, G. The halogen bond. *Chem. Rev.* **2016**, *116*, 2478−2601.
(36) Legon, A. C. The halogen bond: An interim perspective. *Phys. Chem. Chem. Phys.* **2010**, *12*, 7736−7747.
(37) Wei, Y.; Li, Q.; Li, W.; Cheng, J.; McDowell, S. A. C. Influence of the protonation of pyridine nitrogen on pnicogen bonding: Competition and cooperativity. *Phys. Chem. Chem. Phys.* **2016**, *18*, 11348−11356.
(38) Scheiner, S. On the ability of nitrogen to serve as an electron acceptor in a pnicogen bond. *J. Phys. Chem. A* **2021**, *125*, 10419−10427.
(39) Michalczyk, M.; Malik, M.; Zierkiewicz, W.; Scheiner, S. Experimental and theoretical studies of dimers stabilized by two chalcogen bonds in the presence of a N...N pnicogen bond. *J. Phys. Chem. A* **2021**, *125*, 657−668.
(40) Bauzá, A.; Quiñonero, D.; Deyà, P. M.; Frontera, A. Halogen bonding versus chalcogen and pnicogen bonding: A combined Cambridge structural database and theoretical study. *Crystengcomm* **2013**, *15*, 3137−3144.
(41) Jiao, Y.; Liu, Y.; Zhao, W.; Wang, Z.; Ding, X.; Liu, H.; Lu, T. Theoretical study on the interactions of halogen-bonds and pnicogen-bonds in phosphine derivatives with Br2, BrCl, and BrF. *Int. J. Quantum Chem.* **2017**, *117*, No. e25443.
(42) Zhang, Z.; Lu, T.; Ding, L.; Wang, G.; Wang, Z.; Zheng, B.; Liu, Y.; Ding, X. L. Cooperativity effects between regium-bonding and pnicogen-bonding interactions in ternary MF···PH3O···MF (M = Cu, Ag, Au): an ab initio study. *Mol. Phys.* **2020**, *118*, No. e1784478.
(43) Mahapatra, N.; Chandra, S.; Ramanathan, N.; Sundararajan, K. Experimental proof for σ and π-hole driven dual pnicogen bonding in phosphoryl chloride-nitromethane heterodimers: A combined matrix isolation infrared and ab initio computational studies. *J. Mol. Struct.* **2022**, *1251*, 132045.
(44) De Vleeschouwer, F.; De Proft, F.; Ergün, Ö.; Herrebout, W.; Geerlings, P. A combined experimental/quantum-chemical study of tetrel, pnictogen, and chalcogen bonds of linear triatomic molecules. *Molecules* **2021**, *26*, 6767.
(45) Chandra, S.; Suryaprasad, B.; Ramanathan, N.; Sundararajan, K. Nitrogen as a pnicogen?: Evidence for pi-hole driven novel pnicogen bonding interactions in nitromethane-ammonia aggregates using matrix isolation infrared spectroscopy and ab initio computations. *Phys. Chem. Chem. Phys.* **2021**, *23*, 6286−6297.
(46) Frontera, A.; Bauza, A. On the importance of pnictogen and chalcogen bonding interactions in supramolecular catalysis. *Int. J. Mol. Sci.* **2021**, *22*, 12550.
(47) Del Bene, J. E.; Alkorta, I.; Sanchez-Sanz, G.; Elguero, J. 31P−31P spin−spin coupling constants for pnicogen homodimers. *Chem. Phys. Lett.* **2011**, *512*, 184−187.
(48) Humeniuk, H. V.; Gini, A.; Hao, X.; Coelho, F.; Sakai, N.; Matile, S. Pnictogen-bonding catalysis and transport combined: Polyether transporters made in situ. *JACS Au* **2021**, *1*, 1588−1593.
(49) Bauzá, A.; Quiñonero, D.; Deyà, P. M.; Frontera, A. Pnicogen-pi complexes: Theoretical study and biological implications. *Phys. Chem. Chem. Phys.* **2012**, *14*, 14061−14066.
(50) Politzer, P.; Murray, J. S.; Concha, M. C. σ-hole bonding between like atoms; a fallacy of atomic charges. *J. Mol. Model.* **2008**, *14*, 659−665.
(51) Lu, Y.; Zou, J.; Wang, H.; Yu, Q.; Zhang, H.; Jiang, Y. Triangular halogen trimers. A DFT study of the structure, cooperativity, and vibrational properties. *J. Phys. Chem. A* **2005**, *109*, 11956−11961.
(52) Pedireddi, V. R.; Reddy, D. S.; Goud, B. S.; Craig, D. C.; Rae, A. D.; Desiraju, G. R. The nature of halogen...halogen interactions and the crystal-structure of 1,3,5,7-tetraiodoadamantane. *J. Chem. Soc., Perkin Trans. 2* **1994**, *11*, 2353−2360.
(53) Sarma, J. A. R. P.; Desiraju, G. R. The role of Cl...Cl and C-H...O interactions in the crystal engineering of 4-.ANG. short-axis structures. *Acc. Chem. Res.* **2002**, *19*, 222−228.
(54) Varadwaj, A.; Marques, H.; Varadwaj, P. Is the fluorine in molecules dispersive? Is molecular electrostatic potential a valid property to explore fluorine-centered non-covalent interactions? *Molecules* **2019**, *24*, 379−407.
(55) Varadwaj, P.; Varadwaj, A.; Marques, H. Halogen bonding: A halogen-centered noncovalent interaction yet to be understood. *Inorganics* **2019**, *7*, 40−102.
(56) Zhao, T.; Zhou, J.; Wang, Q.; Jena, P. Like charges attract? *J. Phys. Chem. Lett.* **2016**, *7*, 2689−2695.
(57) Varadwaj, A.; Varadwaj, P. R.; Yamashita, K. Do surfaces of positive electrostatic potential on different halogen derivatives in molecules attract? like attracting like. *J. Comput. Chem.* **2018**, *39*, 343−350.
(58) Varadwaj, A.; Marques, H. M.; Varadwaj, P. R. Nature of halogen-centered intermolecular interactions in crystal growth and design: Fluorine-centered interactions in dimers in crystalline

https://doi.org/10.1021/acsomega.2c00176
ACS Omega 2022, 7, 11264−11275

hexafluoropropylene as a prototype. *J. Comput. Chem.* **2019**, *40*, 1836−1860.
(59) Varadwaj, A.; Varadwaj, P. R.; Marques, H. M.; Yamashita, K. Revealing factors influencing the fluorine-centered non-covalent interactions in some fluorine-substituted molecular complexes: Insights from first-principles studies. *ChemPhysChem* **2018**, *19*, 1486−1499.
(60) Echeverría, J.; Velásquez, J. D.; Alvarez, S. Understanding the interplay of dispersion, charge transfer, and electrostatics in noncovalent interactions: The case of bromine−carbonyl short contacts. *Cryst. Growth Des.* **2020**, *20*, 7180−7187.
(61) Politzer, P.; Riley, K. E.; Bulat, F. A.; Murray, J. S. Perspectives on halogen bonding and other σ-hole interactions: Lex parsimoniae (Occam's Razor). *Comput. Theor. Chem.* **2012**, *998*, 2−8.
(62) Ibrahim, M. A. A.; Shehata, M. N. I.; Soliman, M. E. S.; Moustafa, M. F.; El-Mageed, H. R. A.; Moussa, N. A. M. Unusual chalcogen···chalcogen interactions in like···like and unlike Y=C=Y··· Y=C=Y complexes (Y = O, S, and Se). *Phys. Chem. Chem. Phys.* **2022**, *24*, 3386−3399.
(63) Scheiner, S. The ditetrel bond: Noncovalent bond between neutral tetrel atoms. *Phys. Chem. Chem. Phys.* **2020**, *22*, 16606−16614.
(64) Grabarz, A.; Michalczyk, M.; Zierkiewicz, W.; Scheiner, S. Noncovalent Bonds between Tetrel Atoms. *ChemPhysChem* **2020**, *21*, 1934−1944.
(65) Ibrahim, M. A. A.; Moussa, N. A. M.; Soliman, M. E. S.; Moustafa, M. F.; Al-Fahemi, J. H.; El-Mageed, H. R. A. On the potentiality of X-T-X3 compounds (T = C, Si, and Ge, and X = F, Cl, and Br) as tetrel- and halogen-bond donors. *ACS Omega* **2021**, *6*, 19330−19341.
(66) Yang, Q.; Li, Q.; Scheiner, S. Diboron bonds between BX3 (X=H, F, CH3) and BYZ2 (Y=H, F; Z=CO, N2 , CNH). *ChemPhysChem* **2021**, *22*, 1461−1469.
(67) Bandrauk, A. D.; Sedik, E.-W. S.; Matta, C. F. Laser control of reaction paths in ion−molecule reactions. *Mol. Phys.* **2006**, *104*, 95−102.
(68) Arabi, A. A.; Matta, C. F. Effects of external electric fields on double proton transfer kinetics in the formic acid dimer. *Phys. Chem. Chem. Phys.* **2011**, *13*, 13738−13748.
(69) Xu, H.; Cheng, J.; Li, Q.; Li, W. Some measures for making a traditional halogen bond be chlorine-shared or ion-pair one in FCl•NH3 complex. *Mol. Phys.* **2016**, *114*, 3643−3649.
(70) Tokatlı, A.; Tunc, F.; Ucun, F. Effect of external electric field on C-X ... pi halogen bonds. *J. Mol. Model.* **2019**, *25*, 57.
(71) Ibrahim, M. A. A.; Kamel, A. A. K.; Soliman, M. E. S.; Moustafa, M. F.; El-Mageed, H. R. A.; Taha, F.; Mohamed, L. A.; Moussa, N. A. M. Effect of external electric field on tetrel bonding interactions in (FTF3...FH) complexes (T = C, Si, Ge, and Sn). *ACS Omega* **2021**, *6*, 25476−25485.
(72) Ibrahim, M. A. A.; Saad, S. M. A.; Al-Fahemi, J. H.; Mekhemer, G. A. H.; Ahmed, S. A.; Shawky, A. M.; Moussa, N. A. M. External electric field effects on the σ-hole and lone-pair hole interactions of group V elements: A comparative investigation. *RSC Adv.* **2021**, *11*, 4022−4034.
(73) Møller, C.; Plesset, M. S. Note on an approximation treatment for many-electron systems. *Phys. Rev.* **1934**, *46*, 618−622.
(74) Dunning, T. H. Gaussian basis sets for use in correlated molecular calculations. I. The atoms boron through neon and hydrogen. *J. Chem. Phys.* **1989**, *90*, 1007−1023.
(75) Woon, D. E.; Dunning, T. H. Gaussian basis sets for use in correlated molecular calculations. III. The atoms aluminum through argon. *J. Chem. Phys.* **1993**, *98*, 1358−1371.
(76) Woon, D. E.; Dunning, T. H. Gaussian basis sets for use in correlated molecular calculations. IV. Calculation of static electrical response properties. *J. Chem. Phys.* **1994**, *100*, 2975−2988.
(77) Lu, T.; Chen, F. Multiwfn: a multifunctional wavefunction analyzer. *J. Comput. Chem.* **2012**, *33*, 580−592.
(78) Ibrahim, M. A. A. Molecular mechanical perspective on halogen bonding. *J. Mol. Model.* **2012**, *18*, 4625−4638.
(79) Ibrahim, M. A. A.; Moussa, N. A. M.; Safy, M. E. A. Quantum-mechanical investigation of tetrel bond characteristics based on the point-of-charge (PoC) approach. *J. Mol. Model.* **2018**, *24*, 219.
(80) Ibrahim, M. A. A.; Ahmed, O. A. M.; Moussa, N. A. M.; El-Taher, S.; Moustafa, H. Comparative investigation of interactions of hydrogen, halogen and tetrel bond donors with electron-rich and electron-deficient π-systems. *RSC Adv.* **2019**, *9*, 32811−32820.
(81) Ibrahim, M. A. A.; Telb, E. M. Z. Sigma-hole and lone-pair hole interactions in chalcogen-containing complexes: A comparative study. *ACS Omega* **2020**, *5*, 21631−21640.
(82) Mishra, B. K.; Karthikeyan, S.; Ramanathan, V. Tuning the C-H...Pi interaction by different substitutions in benzene-acetylene complexes. *J. Chem. Theory Comput.* **2012**, *8*, 1935−1942.
(83) Boys, S. F.; Bernardi, F. The calculation of small molecular interactions by the differences of separate total energies. Some procedures with reduced errors. *Mol. Phys.* **1970**, *19*, 553−566.
(84) Bader, R. F. W. Atoms in molecules. *Acc. Chem. Res.* **1985**, *18*, 9−15.
(85) Johnson, E. R.; Keinan, S.; Mori-Sánchez, P.; Contreras-García, J.; Cohen, A. J.; Yang, W. Revealing noncovalent interactions. *J. Am. Chem. Soc.* **2010**, *132*, 6498−6506.
(86) Humphrey, W.; Dalke, A.; Schulten, K. VMD: Visual molecular dynamics. *J. Mol. Graphics* **1996**, *14*, 33−38.
(87) Frisch, M. J.; Trucks, G. W.; Schlegel, H. B.; Scuseria, G. E.; Robb, M. A.; Cheeseman, J. R.; Scalmani, G.; Barone, V.; Mennucci, B.; Petersson, G. A.; Nakatsuji, H.; Caricato, M.; Li, X.; Hratchian, H. P.; Izmaylov, A. F.; Bloino, J.; Zheng, G.; Sonnenberg, J. L.; Hada, M.; Ehara, M.; Toyota, K.; Fukuda, R.; Hasegawa, J.; Ishida, M.; Nakajima, T.; Honda, Y.; Kitao, O.; Nakai, H.; Vreven, T.; Montgomery, J. A.; Peralta, J. E.; Ogliaro, F.; Bearpark, M.; Heyd, J. J.; Brothers, E.; Kudin, K. N.; Staroverov, V. N.; Kobayashi, R.; Normand, J.; Raghavachari, K.; Rendell, A.; Burant, J. C.; Iyengar, S. S.; Tomasi, J.; Cossi, M.; Rega, N.; Millam, J. M.; Klene, M.; Knox, J. E.; Cross, J. B.; Bakken, V.; Adamo, C.; Jaramillo, J.; Gomperts, R.; Stratmann, R. E.; Yazyev, O.; Austin, A. J.; Cammi, R.; Pomelli, C.; Ochterski, J. W.; Martin, R. L.; Morokuma, K.; Zakrzewski, V. G.; Voth, G. A.; Salvador, P.; Dannenberg, J. J.; Dapprich, S.; Daniels, A. D.; Farkas, Ö.; Foresman, J. B.; Ortiz, J. V.; Cioslowski, J.; Fox, D. J. *Gaussian 09*, Revision E01; Gaussian Inc.: Wallingford CT, USA., 2009.
(88) Turney, J. M.; Simmonett, A. C.; Parrish, R. M.; Hohenstein, E. G.; Evangelista, F. A.; Fermann, J. T.; Mintz, B. J.; Burns, L. A.; Wilke, J. J.; Abrams, M. L.; Russ, N. J.; Leininger, M. L.; Janssen, C. L.; Seidl, E. T.; Allen, W. D.; Schaefer, H. F.; King, R. A.; Valeev, E. F.; Sherrill, C. D.; Crawford, T. D. PSI4: An open-source ab initio electronic structure program. *Wiley Interdiscip. Rev.: Comput. Mol. Sci.* **2012**, *2*, 556−565.
(89) Hohenstein, E. G.; Sherrill, C. D. Density fitting of intramonomer correlation effects in symmetry-adapted perturbation theory. *J. Chem. Phys.* **2010**, *133*, 014101.
(90) Parker, T. M.; Burns, L. A.; Parrish, R. M.; Ryno, A. G.; Sherrill, C. D. Levels of symmetry adapted perturbation theory (SAPT). I. Efficiency and performance for interaction energies. *J. Chem. Phys.* **2014**, *140*, 094106.
(91) Lakshminarayanan, S.; Jeyasingh, V.; Murugesan, K.; Selvapalam, N.; Dass, G. Molecular electrostatic potential (MEP) surface analysis of chemo sensors: An extra supporting hand for strength, selectivity & non-traditional interactions. *J. Photochem. Photobiol.* **2021**, *6*, 100022.
(92) Asghar, A.; Bello, M. M.; Raman, A. A. A.; Daud, W. M. A. W.; Ramalingam, A.; Zain, S. B. M. Predicting the degradation potential of acid blue 113 by different oxidants using quantum chemical analysis. *Heliyon* **2019**, *5*, No. e02396.
(93) Kaya Kınaytürk, N.; Kalaycı, T.; Tunalı, B. Experimental and computational investigations on the molecular structure, vibrational spectra, electronic properties, and molecular electrostatic potential analysis of phenylenediamine isomers. *Spectrosc. Lett.* **2021**, *54*, 693−706.

https://doi.org/10.1021/acsomega.2c00176
ACS Omega 2022, 7, 11264−11275

(94) Ibrahim, M. A. A.; Mahmoud, A. H. M.; Moussa, N. A. M. Comparative investigation of ±σ−hole interactions of carbon-containing molecules with Lewis bases, acids and di-halogens. *Chem. Pap.* **2020**, *74*, 3569−3580.
(95) Ibrahim, M. A. A.; Mohamed, Y. A. M.; Abuelliel, H. A. A.; Rady, A. s. S. M.; Soliman, M. E. S.; Ahmed, M. N.; Mohamed, L. A.; Moussa, N. A. M. σ-Hole interactions of tetrahedral group iv−viii lewis acid centers with lewis bases: A comparative study. *ChemistrySelect* **2021**, *6*, 11856−11864.
(96) Ibrahim, M. A. A.; Ahmed, O. A. M.; El-Taher, S.; Al-Fahemi, J. H.; Moussa, N. A. M.; Moustafa, H. Cospatial sigma-hole and lone pair interactions of square-pyramidal pentavalent halogen compounds with pi-systems: A quantum mechanical study. *ACS Omega* **2021**, *6*, 3319−3329.
(97) Ibrahim, M. A. A.; Rady, A.-s. S. M.; Soliman, M. E. S.; Moustafa, M. F.; El-Mageed, H. R. A.; Moussa, N. A. M. π-Hole interactions of group III−VI elements with π-systems and Lewis bases: A comparative study. *Struct. Chem.* **2021**, *33*, 9.
(98) Ibrahim, M. A. A.; Rady, A. s. S. M.; Al-Fahemi, J. H.; Telb, E. M. Z.; Ahmed, S. A.; Shawky, A. M.; Moussa, N. A. M. ±π-Hole Interactions: A Comparative Investigation Based on Boron-Containing Molecules. *ChemistrySelect* **2020**, *5*, 13223−13231.
(99) Ibrahim, M. A. A.; Mohamed, Y. A. M.; Abd Elhafez, H. S. M.; Shehata, M. N. I.; Soliman, M. E. S.; Ahmed, M. N.; Abd El-Mageed, H. R.; Moussa, N. A. M. R(*)-hole interactions of group IV-VII radical-containing molecules: A comparative study. *J. Mol. Graphics Modell.* **2022**, *111*, 108097.
(100) Ibrahim, M. A. A.; Moussa, N. A. M. Unconventional type III halogen...halogen interactions: A quantum mechanical elucidation of sigma-hole...sigma-hole and di-sigma-hole interactions. *ACS Omega* **2020**, *5*, 21824−21835.
(101) Jeziorski, B.; Moszynski, R.; Szalewicz, K. Perturbation-Theory Approach to Intermolecular Potential-Energy Surfaces of Van-Der-Waals Complexes. *Chem. Rev.* **1994**, *94*, 1887−1930.
(102) Patkowski, K. Recent developments in symmetry-adapted perturbation theory. *Wiley Interdiscip. Rev.: Comput. Mol. Sci.* **2020**, *10*, No. e1452.
(103) Panini, P.; Gonnade, R. G.; Chopra, D. Experimental and computational analysis of supramolecular motifs involving Csp2-(aromatic)−F and CF3 groups in organic solids. *New J. Chem.* **2016**, *40*, 4981−5001.
(104) Anisimov, A. A.; Ananyev, I. V. Interatomic exchange-correlation interaction energy from a measure of quantum theory of atoms in molecules topological bonding: A diatomic case. *J. Comput. Chem.* **2020**, *41*, 2213−2222.
(105) Grabowski, S. J. QTAIM characteristics of halogen bond and related interactions. *J. Phys. Chem. A* **2012**, *116*, 1838−1845.
(106) Quiñonero, D.; Garau, C.; Rotger, C.; Frontera, A.; Ballester, P.; Costa, A.; Deyà, P. M. Anion−π interactions: Do they exist? *Angew. Chem., Int. Ed.* **2002**, *41*, 3389−3392.
(107) Lo, R.; Švec, P.; Růžičková, Z.; Růžička, A.; Hobza, P. On the nature of the stabilisation of the E...pi pnicogen bond in the SbCl3...toluene complex. *ChemComm* **2016**, *52*, 3500−3503.

https://doi.org/10.1021/acsomega.2c00176
ACS Omega 2022, 7, 11264−11275